Available online at www.sciencedirect.com
ScienceDirect
Surface Science 601 (2007) 4092–4096
SURFACE SCIENCE
www.elsevier.com/locate/susc

First-principles study of the (0 0 1) surface of cubic $SrZrO_3$

Yuan Xu Wang [a,b,*], Masao Arai [a]

[a] Computational Materials Science Center, National Institute for Materials Science, Tsukuba 305-0044, Japan
[b] Institute for Computational Materials Science, School of Physics and Electronics, Henan University, Kaifeng 475000, People's Republic of China

Available online 18 April 2007

Abstract

Density functional calculations have been used to investigate the (0 0 1) surface of cubic $SrZrO_3$ with both SrO and ZrO_2 termination. Surface structure and electronic structure have been obtained. The SrO surface is found to be similar to its counterpart in $SrTiO_3$, while there are marked differences between the ZrO_2 and TiO_2 terminations in $SrZrO_3$ and $SrTiO_3$, respectively, concerning surface relaxation and rumpling. For the ZrO_2-terminated surface of $SrZrO_3$, the covalency of the interaction between the outmost Zr and the O beneath is enhanced as a result of their bond contraction. The band gap reduction and the presence of the surface states are also discussed in relation with the behavior of the electrostatic potential.

Keywords: *Ab initio* quantum chemical methods and calculations; Surface relaxation and reconstruction; Surface electronic phenomena (work function, surface potential, surface states, etc.)

The ABO_3 perovskite type oxides have attracted great interest as functional materials for their various unique properties in spite of their relatively simple crystal structure. Among them, $SrZrO_3$-based perovskite oxides have been studied because of the interest in their high-temperature protonic conductivity [1] with possible applications in fuel cells and hydrogen sensors [2]. In addition, $SrZrO_3$ still has many characteristics which are suitable for high-voltage and high-reliability capacitor applications. Recently, it has been investigated as a possible candidate material for high-K gate dielectrics [3]. The previous experiments [4] report that $SrZrO_3$ undergos three phase transition: it is orthorhombic with space group *Pnma* below 970 K, and belongs to another orthorhombic space group *Cmcm* between 970 and 1020 K. At 1020 K, it transforms into tetragonal with space group $I4/mcm$. Above 1360 K, it becomes cubic with space group $Pm\bar{3}m$.

The surface and interface have an important effect on their properties and applications. Thus, it is desirable to study the surface of $SrZrO_3$ by experimental and theoretical methods. First-principles methods have been successfully applied to the study of the surface of perovskites [5–8]. However, to our knowledge, there is no theoretical study of the surface properties of $SrZrO_3$ by first-principles calculations. In this paper, we present atomic and electronic structure of the (0 0 1) surface of cubic $SrZrO_3$ (SZO) by the full potential linearized augmented plane wave (FLAPW) method. We chose the cubic phase because it is most extensively studied for other compounds, such as $SrTiO_3$. From the comparison with the surface of cubic $SrTiO_3$, we can deduce how the difference of cation atoms affects surface properties. The studies for other low symmetry phases remain as a future problem.

The calculations presented in this work were performed within the local density approximation (LDA) [9] and the generalized gradient approximation (GGA) [10] to density functional theory (DFT), using the FLAPW method with the WIEN2K code [11]. The atomic sphere radii (R_i) of 1.9, 1.8, and 1.6 a.u., were used for Sr, Zr, and O, respectively. The calculations were iterated to self-consistency with a specified energy convergence criterion of 0.01 mRy. We used a $14 \times 14 \times 2$ mesh for the Brillouin Zone integration that represents 28 k-points in its irreducible part. In our

* Corresponding author. Address: Institute for Computational Materials Science, School of Physics and Electronics, Henan University, Kaifeng 475000, People's Republic of China.
E-mail address: wang.yuanxu@nims.go.jp (Y.X. Wang).

0039-6028/$ - see front matter © 2007 Elsevier B.V. All rights reserved.
doi:10.1016/j.susc.2007.04.067

calculations, two types of terminations were considered: SrO termination and ZrO_2 termination. For the SrO-terminated surface, the slab consists of five SrO layers and four ZrO_2 layers and for the ZrO_2-terminated one, five ZrO_2 layers and four SrO layers. The structure of the (0 0 1) surface for SZO is shown in Fig. 1. In both cases, the slabs with seven-lattice-constant thickness are separated by three lattice constants vacuum region. The super-cells are tetragonal with space group *P4mmm*. For the SrO-terminated surface, the first, second, third, fourth, and central layers are SrO, ZrO_2, SrO, ZrO_2, and SrO, respectively. In case of the ZrO_2-terminated one, the first, second, third, fourth, and central layers are ZrO_2, SrO, ZrO_2, SrO, and ZrO_2, respectively. For both cases, the first layer means the surface layer. During the surface structure optimization, all atoms are fully relaxed with forces less than 2 mRy/a.u. Our calculations show that the vacuum region and the number of layers are large enough for these systems.

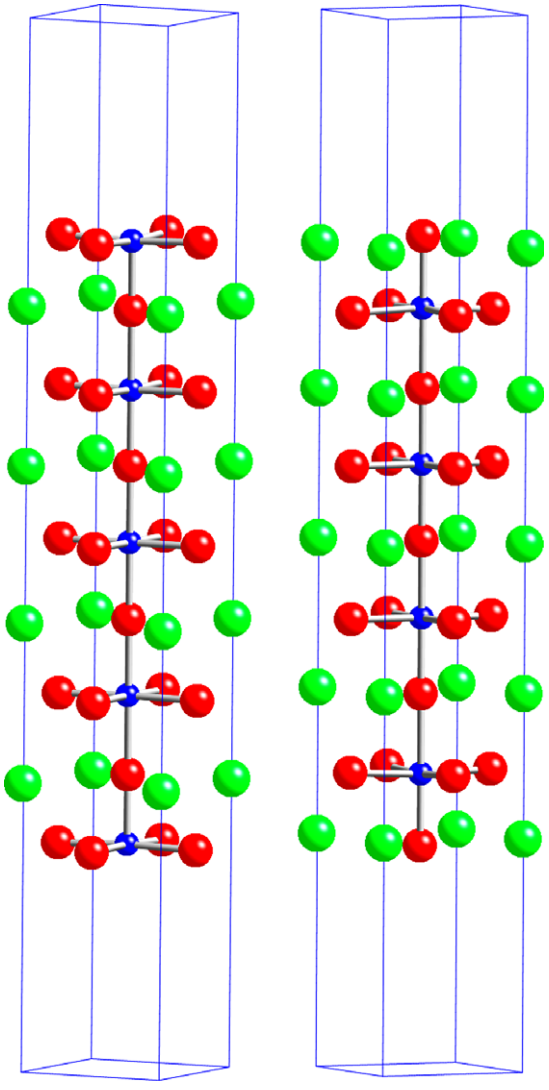

Fig. 1. Structure of (0 0 1) surface of SZO. The left and right figures are the structure of ZrO_2- and SrO-terminated surface. The green, blue, and red color spheres represent the Sr, Zr, and O ions, respectively. (For interpretation of the references in colour in this figure legend, the reader is referred to the web version of this article.)

Before starting the surface calculations, we optimized the bulk structure by the same method and the same computational conditions with a $10\times10\times10$ k-point mesh. The computed lattice constants of cubic SZO with the GGA and the LDA are 4.18 and 4.10 Å, respectively, which are similar to the experimental one, 4.15 Å [4]. We used the theoretical lattice constants in all calculations presented here. Most of the previous DFT studies published for the surface of ABO_3 perovskite materials have been done using the LDA. Previous calculation on the (0 0 1) surface of $SrTiO_3$(STO) shows that the LDA and the GGA predict similar structural relaxations [6]. Generally speaking, the GGA tends to improve upon the LDA in many aspects, especially for atomic and structural energies differences. From our calculated lattice constants for the two materials, it is not clear which approximation is better. Therefore, in our work we investigated the surface of SZO with both the LDA and the GGA.

Tables 1 and 2 show the calculated atomic relaxations at both terminations of the (0 0 1) surface of cubic SZO. For a comparison, the earlier calculations of the cubic STO by the FLAPW [12] method and the plane-wave pseudopotential (PWP) method [8] are also presented. Rumpling parameter s measures the outward displacement of the first-layer oxygen with respect to the first-layer metal atoms, Δd_{12} is the change of the first interlayer spacing, as measured from the surface to the subsurface metal z-coordinate, and similar definition is given to Δd_{23} between the second and third layers. Δd has a characteristic oscillatory behavior (distance contraction between the first and second layers, and dilation between the second and third ones). For the SrO-terminated surface, the surface rumpling in SZO is larger than that in STO, which may be due to the fact that SZO has a larger cell volume than STO. The larger cell volume gives the first-layer Sr atoms more free space and results in its large displacement during the surface relaxation. In the unrelaxed SrO-terminated

Table 1
Calculated atomic displacements (relative to the ideal position) δ_z for the SrO- and ZrO_2-terminated surfaces of SZO

Layer	SrO	δ_z		ZrO_2	δ_z	
		LDA	GGA		LDA	GGA
1	Sr	7.9	7.7	Zr	2.4	3.2
	O	−0.4	−0.2	O	3.2	2.9
2	Zr	−1.5	−1.6	Sr	−3.6	−4.2
	O	−0.3	−0.4	O	−0.4	−0.0
3	Sr	1.6	1.7	Zr	0.5	0.7
	O	−0.1	0.0	O	0.4	0.3
4	Zr	−0.3	−0.4	Sr	−0.6	−0.6
	O	−0.2	−0.3	O	0.0	0.0

Units are in percent of the theoretical lattice constant ($a_0 = 4.10$ and 4.18 Å for LDA and GGA, respectively). δ_z is positive for the displacement toward the bulk.

Table 2
Surface relaxation parameters (in percent of lattice constant a_0) for SZO

	s	Δd_{12}	Δd_{23}
SrO-termination			
SZO–LDA	7.9	−9.1	3.2
SZO–GGA	7.8	−9.3	3.3
STO–LDA–LAPW [12]	5.9	−6.9	2.5
STO–GGA–LAPW [12]	6.0	−7.5	2.7
STO–LDA–PWP [8]	5.8	−6.8	2.4
ZrO_2-termination			
SZO–LDA	−0.7	−6.1	4.2
SZO–GGA	0.3	−7.4	4.9
STO–LDA–LAPW [12]	1.9	−5.9	3.8
STO–GGA–LAPW [12]	2.4	−7.3	4.5
STO–LDA–PWP [8]	1.8	−7.0	3.2

surface, the Sr-O bond length for SZO is 2.96 Å, and larger than that of STO, 2.85 Å, which means that the Sr–O bond length for SZO can get larger reduction than that of STO during the surface relaxation. In case of ZrO_2-termination, the large displacement of the first-layer O atoms results in its small surface rumpling.

The calculated band gap of the ZrO_2-terminated surfaces for SZO with GGA is 3.1 eV, and reduced by comparison with that in the bulk system, 3.3 eV. For the SrO-terminated one, the band gap is 3.3 eV, and similar to bulk. Fig. 2 shows the calculated band structure of SZO. For SrO- and ZrO_2-terminated surfaces structures, the calculated energy bands are uniformly shifted so that 1s core level energy of the metal atom in the central layer is aligned with that in the bulk system. Compared with the bulk system, in the ZrO_2-terminated surface, the states around the valence band maximum tends to extend upward, especially at the M point. From this point of view, it can be considered that the surface state appears at the M point. The upward shift of the valence bands in the ZrO_2-terminated surface is mainly attributed to the states from the first-layer O atoms. Thus, the surface states appearing in the ZrO_2-terminated surface are caused by the first-layer O atoms. The origin of the surface states is attributed to the increase of the electro-static potential near the surface. We estimated an increase of about 0.1 eV from the difference between calculated O 1s level on the top most layer and that on the central layer.

It is interesting to note that the band gap reduction of the ZrO_2-terminated surface is 0.2 eV and much smaller than that of the TiO_2-terminated surface for STO, 0.7 eV. This difference is mainly due to the different increase of the electro-static potential. For the TiO_2-terminated surface of STO, the electro-static potential on the top most layer is about 0.6 eV higher than that on the central layer, which is much larger than that of the ZrO_2-terminated surface layer, 0.1 eV.

Fig. 3 shows the partial density of states (PDOS) of the ZrO_2- and SrO-terminated surface of SZO. From this figure, for the ZrO_2-terminated surface, the first-layer O 2p shifts to the higher energy, which indicates that the band gap reduction of the ZrO_2-terminated surface is mainly due to the upward shift of the first-layer O 2p states. By contrast, the distribution of PDOS for the second-layer O 2p is different from that of the first layer, which indicates that the hybridization between the first-layer Zr 4d and the second-layer O 2p is stronger than that of bulk system. The relaxation of the ZrO_2-terminated surface shortens the bond length between the first-layer Zr atoms and the second layer O atoms, which would enhance the hybridization between them. Fig. 4 plots the charge density corresponding to the O 2p orbitals in the (1 1 0) plane. From this figure, it can be seen that the interaction between the surface-layer Zr and the second-layer O atoms is stronger than the central layer which represents the bulk system.

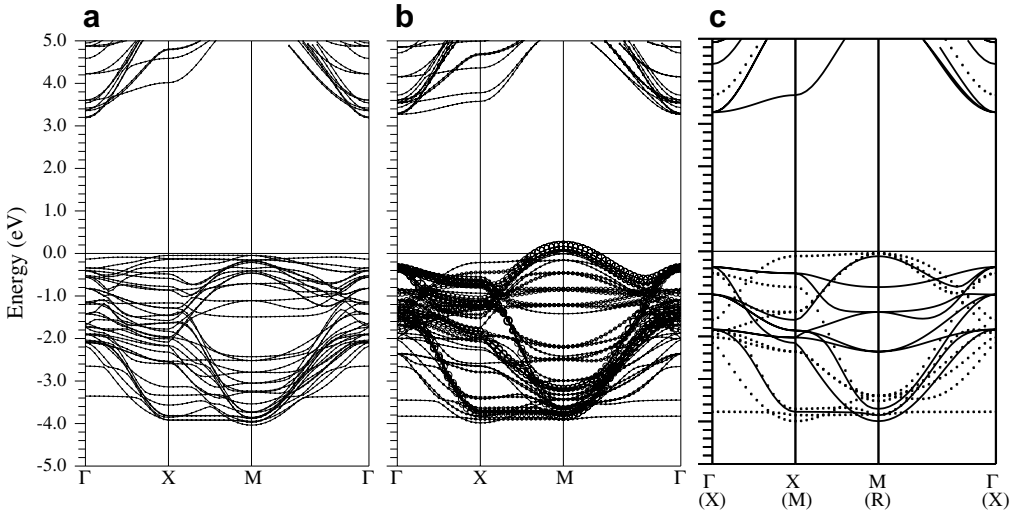

Fig. 2. Band structure of SZO: (a) SrO-terminated surface; (b) ZrO_2-terminated surface of SZO, in which the radii of circles are proportional to the projected weights of the eigenstates on the O atoms in the first layer and (c) bulk, in which the solid and dotted lines represent the band structure on the $\Gamma \to X \to M \to \Gamma$ and $X \to M \to R \to X$ axes, respectively, in the bulk Brillouin.

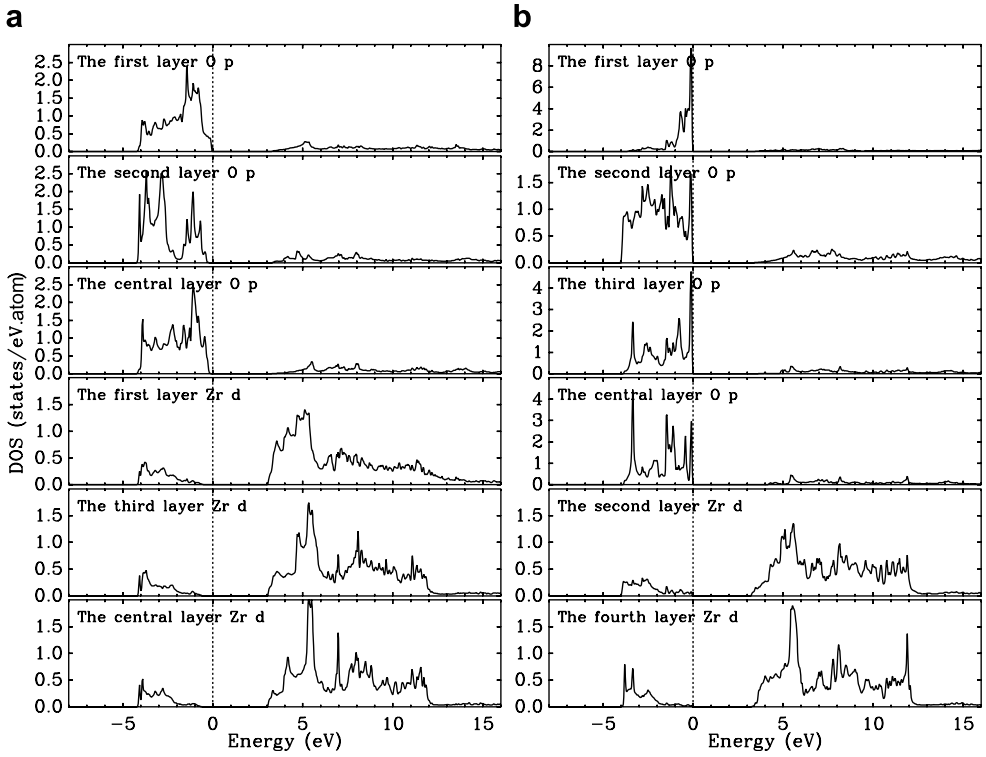

Fig. 3. PDOS of each layer. (a) ZrO_2-terminated surface and (b) SrO-terminated surface.

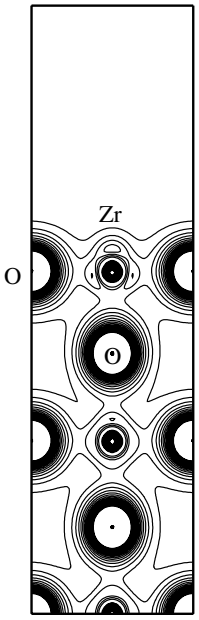

Fig. 4. Charge density contour plot in the (1 1 0) plane corresponding to the energy range of the O 2p bands. The values of the contours in the figure are from 0.1 to 2 e/Å^3 with an increment of 0.1 e/Å^3.

Next, we discuss the surface energy and surface stability. We define E_s to be the average surface energy of two types of surface termination:

$$E_s = \frac{1}{4}[E_{slab}(I) + E_{slab}(II) - 9E_{bulk}], \quad (1)$$

where E_{slab} (I), E_{slab} (II) and E_{bulk} are the total energies of the relaxed SrO-terminated slab, the relaxed ZrO_2-terminated slab, and the bulk crystal per unit cell, respectively. A factor of four comes from the fact that we create four surfaces during cleavage procedure. The number 9 means in our calculations, the two nine layers SrO- and ZrO_2-terminated surfaces represent together nine bulk unit cells. The cleavage energy (E_{cle}) and the relaxation energy (E_{rel}) are defined as

$$E_{cle} = \frac{1}{4}\left[E^{(unrel)}_{slab}(I) + E^{(unrel)}_{slab}(II) - 9E_{bulk}\right], \quad (2)$$

$$E_{rel}(I) = \frac{1}{2}\left[E_{slab}(I) - E^{(unrel)}_{slab}(I)\right], \quad (3)$$

where $E^{(unrel)}_{slab}(I)$, $E^{(unrel)}_{slab}(II)$ and $E_{slab}(I)$ are the total energies for the unrelaxed SrO-terminated slab, the unrelaxed ZrO_2-terminated slab, and the relaxed SrO-terminated slab, respectively. The average surface energy, the cleavage energy and the relaxation energy of SZO and STO are listed in Table 3. The absolute value of the relaxation energy of the ZrO_2-terminated surface for SZO is similar to that of the TiO_2-terminated surface for STO. The surface

Table 3
Theoretical average surface energies for SZO (in eV/Å^2)

	E_{cle}	E_{rel}(I)	E_{rel}(II)	E_s
SZO–GGA	1.56	−0.31	−0.17	0.076
STO–GGA	1.18	−0.19	−0.18	0.064

The E_{cle} (in eV) means the cleavage energy and the E_{rel} (in eV) is the relaxation energy.

energy of SZO is larger than that of STO. A smaller surface energy means easier cleavability under the condition that migration of atoms can be neglected. Thus, the surface of SZO is more difficult to be constructed.

In summary, we found that the surface rumpling of the ZrO_2-terminated surface for SZO is much smaller than that for STO, which is mainly due to the large displacement of the first-layer O atoms in SZO. The rumpling of the SrO-terminated surface structure for SZO is stronger than that for STO. The different surface relaxation behavior of the two materials may be due to the different cell volumes of the two materials. The appearance of the surface states in the case of the ZrO_2-terminated surface is mainly due to an increase of the electro-static potential near the surface. The band gap reduction of the ZrO_2-terminated surface is much smaller than that of the TiO_2-terminated surface of STO, which is mainly due to the different increase of the electro-static potential near the surface. For the ZrO_2-terminated surface, the PDOS results shows that the bond covalency between the first-layer Zr atoms and the second-layer O atoms is enhanced, which is originated from the shortening of their bond length during the surface relaxation.

The calculations were performed on the Numerical Materials simulator at the National Institute for Materials Science. This work is financially supported by Japanese Society for Promotion of Science (JSPS).

References

[1] H. Iwahara, T. Esaka, H. Uchida, N. Maeda, Solid State Ionics 3/4 (1981) 359.
[2] T. Matsuda, S. Yamanaka, K. Kurosaki, Shin-Ichi Kobayashi, J. Alloys Compd. 351 (2003) 43.
[3] C. Chen, W. Zhu, T. Yu, X. Chen, X. Yao, Appl. Surf. Sci. 211 (2003) 244.
[4] B.J. Kennedy, C.J. Howard, B.C. Chakoumakos, Phys. Rev. B 59 (1999) 4023.
[5] J. Padilla, D. Vanderbilt, Phys. Rev. B 56 (1997) 1625.
[6] J.A. Rodriguez, J. García, L. González, Chem. Phys. Lett. 365 (2002) 380.
[7] S. Piskunov, E.A. Kotomin, E. Heifets, J. Maier, R.I. Eglitis, G. Borstel, Surf. Sci. 575 (2005) 75.
[8] B. Meyer, J. Padilla, D. Vanderbilt, Faraday Discuss. 114 (1999) 395.
[9] J.P. Perdew, Y. Wang, Phys. Rev. B 45 (1992) 13244.
[10] J.P. Perdew, K. Burke, M. Ernzerhof, Phys. Rev. Lett. 77 (1996) 3865.
[11] P. Blaha, K. Schwarz, G.K.H. Madsen, D. Kvasnicka, J. Luitz, in: K. Schwarz (Ed.), WIEN2K, An Augmented Plane Wave + Local Orbitals Program for Calculating Crystal Properties, TU Wien, Austria, 2001, ISBN 3-9501031-1-2.
[12] Y.X. Wang, C.L. Wang, W.L. Zhong, J. Phys. Chem. B 109 (2005) 12909.